

String-based parametrization of nucleon GPDs at any skewness: a comparison to lattice QCD

Kiminad A. Mamo*

Physics Department, William & Mary, Williamsburg, VA 23187, USA

Ismail Zahed†

*Center for Nuclear Theory, Department of Physics and Astronomy,
Stony Brook University, Stony Brook, New York 11794-3800, USA*

(Dated: May 24, 2024)

We introduce a string-based parametrization for nucleon quark and gluon generalized parton distributions (GPDs) effective across all skewness values. The conformal moments of the GPDs are expressed as sums of the spin- j nucleon A-form factor, and the skewness-dependent spin- j nucleon D-form factor. This representation, which fulfills the polynomiality condition and does not rely on model-specific assumptions, is derived from t -channel string exchanges in AdS spaces. The spin- j nucleon D-form factor is closely related to the the spin- j nucleon A-form factor. We use the Mellin moments from empirical parton distributions to model the spin- j nucleon A-form factors. Using only five Regge slope parameters, fixed from the electromagnetic and gravitational form factors, our string-based parametrization generates accurate singlet, non-singlet, isovector, and flavor-separated nucleon quark GPDs, along with symmetric nucleon gluon GPDs from their Mellin-Barnes integral representations. Our isovector nucleon quark GPD is in agreement with existing lattice data. Our string-based parametrization should enhance the empirical extraction and global analysis of nucleon GPDs in exclusive processes, bypassing the de-convolution problem.

I. INTRODUCTION

On the light front hadrons are assemblies of valence and sea partons. These constituents, directly probed through hard inclusive and semi-inclusive processes, owe their "visibility" to relativistic time dilation and asymptotic freedom [1–3]. This allows for the separation of hard processes into calculable perturbative factors, and non-perturbative matrix elements like parton distribution functions (PDFs) and fragmentation functions (FFs), the central tenets in modern high-energy scattering data [4, 5].

At the center of our investigation are the Generalized Parton Distributions (GPDs), extended PDFs as off-forward matrix elements of leading twist QCD operators in highly boosted hadron states [6–12], see [13–15] for review. These distributions are inherently non-perturbative. They offer a multi-dimensional view of nucleons, describing their spin, mass and mechanical structure via the variables x , η , and t —respectively representing the parton momentum fraction, skewness, and total momentum transfer [13–15].

Despite their richness, GPDs elude easy probing through first principle QCD lattice simulations, owing to their inherent light cone structure. Yet,

progress has been recently made by recent lattice QCD collaborations [16–23], using the theoretical considerations proposed initially in [24–26], and since extended by others [27, 28]. A number of experiments at various electron facilities [29] are currently under way to shed more light on the phenomenology of GPDs [30, 31], with more systematic exploration anticipated at the forthcoming EIC (electron-ion collider) facility [32–34].

GPDs at finite skewness, have been modeled in various theoretical frameworks, owing to their central role in describing the internal structure of hadrons. These include standard quark models [35–39], chiral soliton models [12, 40, 41], AdS/QCD models [42–44], light front and holography hybrid models [45–50], light front models [51, 52], double distribution models [12, 53–62], conformal moment based models at small skewness [63–73], and recently using lattice data for Compton form factors [74].

The unpolarized GPD $H(x, \eta, t)$ and polarized GPD $\tilde{H}(x, \eta, t)$, are generalized form factors. These distributions reduce to ordinary PDFs in the forward limit, and turn into pertinent Compton form factors when summed over x . The inherent complexity and non-uniqueness in the de-convolution of GPDs from the Compton form factors of deep virtual Compton scattering (DVCS) and deep virtual meson production (DVMP), presents a significant theoretical challenge for their model independent extraction from data [75].

Characteristically, for a fixed Mandelstam t and positive skewness η , GPDs exhibit distinct behaviors

* kamamo@wm.edu

† ismail.zahed@stonybrook.edu

in two kinematic regimes: the DGLAP regime for $|x| > \eta$ and the ERBL regime for $|x| < \eta$. In the DGLAP regime, the dynamics correspond to either quark or antiquark momentum redistribution, while in the ERBL regime, it is akin to the emission of meson-like quark-antiquark pairs [13, 14].

We propose to use the holographic string-based approach (see the review [76], and references therein), to leverage the holographic principle to bypass the de-convolution issue entirely. By employing Gegenbauer moments with fixed conformal spin- j , each moment is directly mapped to its gravity dual, allowing a detailed reconstruction of the GPDs in the ERBL regime, as we noted recently [77]. This method not only simplifies the encoding of stringy properties of QCD at low resolution, but also aligns with empirical Regge phenomenology and Veneziano amplitudes, capturing critical aspects of QCD dispersive analysis such as crossing symmetry, unitarity, and spectral densities in a framework with remarkably few parameters, e.g. open and closed string intercepts and slopes. The GPDs are then expressed through an expansion in integer-valued spin- n conformal moments of quark and gluon PDFs, structured using an orthogonal basis of conformal partial waves (PWs). By employing the Sommerfeld-Watson transform, this series is transformed into an integral over analytically continued complex spin- j conformal moments, which preserves analyticity across all regions of skewness [65].

The outline of the paper is as follows: Section II elaborates on the expansion of quark and gluon GPDs in conformal PWs, particularly in the ERBL region, and discusses their analytical continuation to DGLAP region. Section III details the holographic string parametrization of the conformal moments used for reconstructing the quark and gluon GPDs across all values of parton- x . Section IV compares the conformal moments and the reconstructed GPDs to those derived from Euclidean lattice simulations within the large momentum effective theory (LaMET). Finally, Section V summarizes our findings and conclusions. The appendix provides an overview of the empirical nucleon MSTW PDFs used in our analysis.

II. QUARK AND GLUON GPDS

A natural organization of the quark and gluon GPDs in the ERBL regime, is a series expansion in terms of the conformal partial waves (PWs), with the conformal moments as coefficients. The conformal PWs are Gegenbauer polynomials in parton- x of the struck quark in the GPD, that diagonalize the pertinent GPD evolution operator. The conformal moments carry the essential dynamics of the quarks and gluons in hadrons.

The extension to the DGLAP regime requires analytical continuation of the series expansion, using a Sommerfeld-Watson transform. The result is a GPD given as an integral transform of spin- j conformal moments, following a pertinent analytical continuation of the PWs. In this section we recall the essential relations needed in this continuation, for both the quarks and gluons.

A. Quark GPDs

The quark GPDs, defined as $H_q(x, \eta, t; \mu)$, can be naturally expanded in terms of Gegenbauer polynomials in parton- x . These polynomials are best structured in terms of PWs which are eigenstates of the pertinent QCD evolution operator for a given GPD.

1. Series expansion

More specifically, a generic quark GPD admits a series expansion for $|x| < \eta$

$$H_q(x, \eta, t; \mu) = \sum_{n=1}^{\infty} (-1)^{n-1} p_n(x, \eta) \mathbb{F}_q(n, \eta, t; \mu), \quad (1)$$

with the conformal moments $\mathbb{F}_q(n, \eta, t; \mu)$ as coefficient functions. The conformal partial waves (PWs), $p_n(x, \eta)$, form an orthonormal basis set defined as

$$p_n(x, \eta) = \frac{1}{\eta^n} p_n\left(\frac{x}{\eta}\right) \quad \text{with} \quad p_n(x) = \theta(1 - |x|) \frac{2^{n-1} \Gamma(3/2 + n)}{\Gamma(3/2) \Gamma(2 + n)} (1 - x^2) C_{n-1}^{3/2}(-x), \quad (2)$$

where $C_n^\nu(x)$ are Gegenbauer polynomials. The PWs encode reflection symmetry $p_n(-x, \eta) = (-1)^n p_n(x, \eta)$, and turn to distributions at zero

skewness

$$p_n(x, \eta = 0) = \frac{1}{n!} \delta^{(n)}(x). \quad (3)$$

The orthonormality relation of Gegenbauer polynomials, key to the inversion of the GPDs, is captured by

$$\int_{-1}^1 dx c_{n'}(x, \eta) p_n(x, \eta) = (-1)^{n-1} \delta_{n'n}, \quad (4)$$

where

$$\begin{aligned} c_n(x, \eta) &= \eta^{n-1} \times c_j\left(\frac{x}{\eta}\right) \\ c_n(x) &= \frac{\Gamma(3/2)\Gamma(n)}{2^{n-1}\Gamma(1/2+n)} \times C_{n-1}^{3/2}(x), \end{aligned} \quad (5)$$

$$H_q^{(-)}(x, \eta, t; \mu) = H_q(x, \eta, t; \mu) + H_q(-x, \eta, t; \mu) = \sum_{n=1}^{\infty} (-1)^{n-1} (p_n(x, \eta) + p_n(-x, \eta)) \mathbb{F}_q^{(-)}(n, \eta, t; \mu), \quad (8)$$

for odd $n = 1, 3, \dots$, with support $0 \leq x \leq \eta$. (8) can be extended to the complex j -plane with the help of the Sommerfeld-Watson integral transform, with support $0 \leq x \leq 1$, as

$$\begin{aligned} H_q^{(-)}(x, \eta, t; \mu) &= \\ \frac{1}{2i} \int_{\mathbb{C}} dj \frac{1}{\sin(\pi j)} (p_j(x, \eta) + p_j(-x, \eta)) \mathbb{F}_q^{(-)}(j, \eta, t; \mu), \end{aligned} \quad (9)$$

by extending spin- n to complex spin- j , as suggested in [65] (for recent discussions see [71] and references

Note that the conformal moments are Gegenbauer moments of the GPD

$$\mathbb{F}_q(n, \eta, t; \mu^2) = \int_{-1}^1 dx c_n(x, \eta) H_q(x, \eta, t; \mu), \quad (6)$$

for $n = 1, 2, \dots$. Also note that in the forward limit, the spin- n conformal moments of the quark GPDs reduce to the spin- n Mellin moments of the quark GPDs, since

$$\lim_{\eta \rightarrow 0} c_n(x, \eta) = x^{n-1}. \quad (7)$$

2. Non-singlet (Valence) Quark GPDs

The non-singlet or valence quark GPDs, denoted as $H_q^{(-)}(x, \eta, t; \mu)$, represent the difference between quark distributions and their antiparticle counterparts within the hadron. This difference is key for understanding the valence quark structure. They are defined as

therein). Note that the factor $\frac{1}{\sin(\pi j)}$, with residues $\text{Res}_{j=n} 1/\sin(\pi j) = (-1)^{n-1}/\pi$ for $n = 1, 3, \dots$, yields the original series, barring additional singularities within the integration contour \mathbb{C} .

The analytic continuation of the PWs $p_n(x, \eta)$ to the complex j -plane, can be done using their Schläfli integral representation [65]

$$\begin{aligned} p_j(x, \eta) &= \\ \theta(\eta - |x|) \frac{1}{\eta^j} \mathcal{P}_j\left(\frac{x}{\eta}\right) + \theta(x - \eta) \frac{1}{x^j} \mathcal{Q}_j\left(\frac{x}{\eta}\right) \end{aligned} \quad (10)$$

The functions \mathcal{P}_j and \mathcal{Q}_j are hypergeometric functions

$$\begin{aligned} \mathcal{P}_j\left(\frac{x}{\eta}\right) &= \left(1 + \frac{x}{\eta}\right) {}_2F_1\left(-j, j+1, 2 \middle| \frac{1}{2} \left(1 + \frac{x}{\eta}\right)\right) \times \frac{2^j \Gamma(3/2 + j)}{\Gamma(1/2) \Gamma(j)}, \\ \mathcal{Q}_j\left(\frac{x}{\eta}\right) &= {}_2F_1\left(\frac{j}{2}, \frac{j+1}{2}; \frac{3}{2} + j \middle| \frac{\eta^2}{x^2}\right) \times \frac{\sin(\pi j)}{\pi}, \end{aligned} \quad (11)$$

for all values of parton- x . The complex-valued func-

tions \mathcal{P}_j cover the ERBL regime, and \mathcal{Q}_j cover the

DGLAP regime. This illustrates how the analytic continuation process for the PWs is captured in the complex spin- j plane. Note that the functional dependence of the conformal moment $\mathbb{F}_q(j, \eta, t; \mu)$ is common to both regimes, which makes it accessible from the ERBL regime using dual gravity. This observation is central to our analysis. The conformal moments carry the essential hadron dynamics, that interpolate between the distribution amplitudes (ERBL regime) and the parton distribution functions (DGLAP regime). To segregate between the contributions stemming from valence and sea quarks partonic distributions in hadrons, we now discuss the singlet and non-singlet quark GPDs.

3. Non-singlet (Isovector) Quark GPDs

The non-singlet isovector quark GPDs, denoted as $H_{u-d}^{(-)}(x, \eta, t; \mu)$, represents the difference between the up and down quark distributions. They are de-

$$H^{(+)}(x, \eta, t; \mu) = \sum_{q=1}^{N_f} H_q(x, \eta, t; \mu) - H_q(-x, \eta, t; \mu) = \sum_{n=2}^{\infty} (-1)^{n-1} (p_n(x, \eta) - p_n(-x, \eta)) \sum_{q=1}^{N_f} \mathbb{F}_q^{+}(j, \eta, t; \mu), \quad (14)$$

for even $n = 2, 4, \dots$. Similarly to the non-singlet case, we use the the Sommerfeld-Watson transform to extend (14) to complex conform spin- j with support $0 \leq x \leq 1$

$$H^{(+)}(x, \eta, t; \mu) = \frac{1}{2i} \int_{\mathbb{C}} dj \frac{1}{\sin(\pi j)} (p_j(x, \eta) - p_j(-x, \eta)) \sum_{q=1}^{N_f} \mathbb{F}_q^{+}(j, \eta, t; \mu), \quad (15)$$

B. Gluon GPDs

Following our brief discussion of the quark GPDs, we now present the gluon GPDs. Generically, the gluons whether in perturbative or non-perturbative form, are blind to the electric and weak probes, and hence more subtle to quantify. Yet, they are essential ingredients in the composition of the mass and spin of hadrons.

defined as

$$H_{u-d}^{(-)}(x, \eta, t; \mu) = \sum_{n=1}^{\infty} (-1)^{n-1} p_n(x, \eta) \mathbb{F}_{u-d}^{(-)}(n, \eta, t; \mu), \quad (12)$$

for all $n = 1, 2, 3, 4, \dots$. To account for non-integer conformal spins, (12) can be extended to the complex j -plane with the help of the Sommerfeld-Watson integral transform with support $-\eta \leq x \leq 1$

$$H_{u-d}^{(-)}(x, \eta, t; \mu) = \frac{1}{2i} \int_{\mathbb{C}} dj \frac{1}{\sin(\pi j)} p_j(x, \eta) \mathbb{F}_{u-d}^{(-)}(j, \eta, t; \mu), \quad (13)$$

with the analytically continued conformal PWs $p_j(x, \eta)$ given in (10).

4. Singlet (Sea) Quark GPDs

The singlet or sea quark GPDs, $H^{(+)}(x, \eta, t; \mu)$, sum the contributions from all quark flavors, encompassing both quarks and antiquarks. They reflect on the sea quark distribution. The singlet combination is defined as

1. Series expansion

The formulation of the gluon GPDs, $H_g(x, \eta, t; \mu)$, mirrors that for the quarks, albeit with adaptations to account for the unique characteristics of gluons. The series expansion of the gluon GPDs, in terms of their spin- n conformal moments $\mathbb{F}_g(n, \eta, t; \mu)$, is

$$H_g(x, \eta, t; \mu) = \sum_{n=2}^{\infty} (-1)^{n+1} g p_n(x, \eta) \mathbb{F}_g(n, \eta, t; \mu), \quad (16)$$

with the sum running now unrestricted. The gluon PWs ${}^g p_n(x, \eta)$, form the basis functions for the gluon partonic distributions in hadrons

$$\begin{aligned} {}^g p_n(x, \eta) &= \frac{1}{\eta^{n-1}} {}^g p_n\left(\frac{x}{\eta}\right) \\ {}^g p_n(x) &= (-1)\theta(1-|x|) \frac{2^{n-1} 3^2 \Gamma(3/2+n)}{\Gamma(5/2)\Gamma(3+n)} (1-x^2)^2 C_{n-2}^{5/2}(-x), \end{aligned} \quad (17)$$

with the reflection symmetry

$${}^g p_n(-x, \eta) = (-1)^n {}^g p_n(x, \eta).$$

The orthogonality relation for the Gegenbauer polynomials, key for the inversion process, is

$$\int_{-1}^1 dx {}^g c_{n'}(x, \eta) {}^g p_n(x, \eta) = (-1)^{1+n} \delta_{n'n}, \quad (18)$$

which ensures that

$$\mathbb{F}^g(n, \eta, t; \mu) = \int_{-1}^1 dx {}^g c_n(x, \eta) H^g(x, \eta, t; \mu), \quad (19)$$

for $n = 2, 3, \dots$, with

$$\begin{aligned} {}^g c_n(x, \eta) &= \eta^{n-2} \times {}^g c_j\left(\frac{x}{\eta}\right) \\ {}^g c_n(x) &= \frac{\Gamma(5/2)\Gamma(n-1)}{2^{n-2}\Gamma(1/2+n)} \times C_{n-2}^{5/2}(x). \end{aligned} \quad (20)$$

Note that in the forward limit, the spin- n conformal moments of the gluon GPDs reduce to the spin- n

Mellin moments of gluon GPDs since

$$\lim_{\eta \rightarrow 0} {}^g c_n(x, \eta) = x^{n-2}. \quad (21)$$

2. Integral transform

Similarly to the quark GPDs, the series expansion for the gluon GPD can be analytically continued from real spin- n to complex spin- j using the Sommerfeld-Watson transform as originally suggested in [65]. The resulting Mellin-Barnes integral representation of the gluon GPD is

$$\begin{aligned} H_g(x, \eta, t; \mu) &= \\ &= \frac{1}{2i} \int_{\mathbb{C}} dj \frac{(-1)}{\sin(\pi j)} {}^g p_j(x, \eta) \mathbb{F}_g(j, \eta, t; \mu^2), \end{aligned} \quad (22)$$

where the factor $\frac{1}{\sin(\pi j)}$ is included to ensure proper normalization, and the recovery of the PWs expansion in the absence of other singularities within the contour \mathbb{C} . The analytically continued gluon PWs are

$$\begin{aligned} {}^g p_j(x, \eta) &= \\ &= \theta(\eta - |x|) \frac{1}{\eta^{j-1}} {}^g \mathcal{P}_j\left(\frac{x}{\eta}\right) + \theta(x - \eta) \frac{1}{x^{j-1}} {}^g \mathcal{Q}_j\left(\frac{x}{\eta}\right), \end{aligned} \quad (23)$$

where the functions ${}^g \mathcal{P}_j$ and ${}^g \mathcal{Q}_j$ are given by

$$\begin{aligned} {}^g \mathcal{P}_j\left(\frac{x}{\eta}\right) &= \left(1 + \frac{x}{\eta}\right)^2 {}_2F_1\left(-j, j+1, 3 \left| \frac{1}{2} \left(1 + \frac{x}{\eta}\right)\right.\right) \frac{2^{j-1} \Gamma(3/2+j)}{\Gamma(1/2)\Gamma(j-1)}, \\ {}^g \mathcal{Q}_j\left(\frac{x}{\eta}\right) &= {}_2F_1\left(\frac{j-1}{2}, \frac{j}{2}; \frac{3}{2} + j; \frac{\eta^2}{x^2}\right) \frac{\sin(\pi[j+1])}{\pi}, \end{aligned} \quad (24)$$

The spin-averaged gluon GPD is captured by the

symmetric combination $H_g^{(+)}(x, \eta, t; \mu)$,

$$H_g^{(+)}(x, \eta, t; \mu) = H_g(x, \eta, t; \mu) + H_g(-x, \eta, t; \mu) = \sum_{n=2}^{\infty} (-1)^{n+1} (g_{p_n}(x, \eta) + g_{p_n}(-x, \eta)) \mathbb{F}_g^{(+)}(j, \eta, t; \mu), \quad (25)$$

where the sum runs over even $n = 2, 4, \dots$. Its analytical continuation to complex spin- j , using the Sommerfeld-Watson transform, with support $0 \leq x \leq 1$, is given by

$$H_g^{(+)}(x, \eta, t; \mu) = \frac{1}{2i} \int_{\mathbb{C}} dj \frac{(-1)^j}{\sin(\pi j)} (g_{p_j}(x, \eta) + g_{p_j}(-x, \eta)) \mathbb{F}_g^{(+)}(j, \eta, t; \mu), \quad (26)$$

with the conformal PWs $g_{p_j}(x, \eta)$ defined in (23).

III. CONFORMAL MOMENTS OF GPDS USING THE STRING-BASED PARAMETRIZATION

The holographic approach to the space-like form factors in QCD is string based. For a fixed boundary source, the form factor follows from the bulk-to-boundary propagator which naturally resums the Reggeized states in bulk. Similarly, the holographic description of scattering amplitudes in the Regge limit, is well described by the resummed spin- j exchanges in bulk, readily capturing the subtle aspects of the multi-parton exchanges in the ERBL regime for quarks through open strings, and for gluons through closed strings.

In our recent holographic analysis of the GPDs at finite skewness [77], we have shown how most of the GPDs involved in exclusive processes can be obtained holographically in the ERBL regime, where the string based description with its symmetries and dualities, is dominant. A string based parametrization for the conformal moments was derived in this regime where $|x| < \eta$. The chief idea of this work is to show how this string based parametrization for the conformal spin- j moments can be extended to the DGLAP regime for any skewness, using the analytical continuation of the PWs expansion we detailed above.

A. Quarks conformal moments: non-singlet-valence-isovector

Using dual gravity, the conformal moments of the non-singlet (valence) quark GPDs, were explicitly derived by us in [77]. As we noted earlier, their functional dependence in j, η holds whatever the regime. More specifically, the non-singlet quark conformal moments at the resolution $\mu = \mu_0$ are represented by the valence quark spin- j A-form factor as [77]

$$\mathbb{F}_q^{(-)}(j, \eta, t; \mu_0) = \mathcal{F}_q^{(-)}(j, t; \mu_0), \quad (27)$$

for odd $j = 1, 3, \dots$, which is tied to the valence (non-singlet) quark PDF through

$$\mathcal{F}_q^{(-)}(j, t; \mu_0) = \int_0^1 dx \frac{q_v(x; \mu_0)}{x^{1-j+\alpha'_{(-)}t}}, \quad (28)$$

with $q_v(x; \mu_0) = q(x; \mu_0) - \bar{q}(x; \mu_0) = H_q^{(-)}(x, \eta = 0, t = 0; \mu_0)$ at $\mu = \mu_0$. Note that in (27), we have ignored the valence quark skewness-dependent spin- j D-form factor which is vanishing. We can also write

$$\begin{aligned} \mathbb{F}_{u\pm d}^{(-)}(j, \eta, t; \mu_0) &= \mathcal{F}_{u\pm d}^{(-)}(j, t; \mu_0) \\ &= \int_0^1 dx \frac{u_v(x; \mu_0) \pm d_v(x; \mu_0)}{x^{1-j+\alpha'_{u\pm d}t}}, \end{aligned} \quad (29)$$

assuming $\bar{u}(x, \mu_0) = \bar{d}(x, \mu_0)$. We can fix $\alpha'_{u\pm d}$, using the experimental Dirac electromagnetic form factor of the proton ($F_{1p}(t)$) and neutron ($F_{1n}(t)$) from their valence combination

$$\mathcal{F}_{u+d}^{(-)}(j = 1, t; \mu_0) = 3(F_{1p}(t) + F_{1n}(t)), \quad (30)$$

and the isovector combination

$$\mathcal{F}_{u-d}^{(-)}(j = 1, t; \mu_0) = F_{1p}(t) - F_{1n}(t). \quad (31)$$

We specifically use the experimental Dirac electromagnetic form factor of the nucleon from [78].

Note that for $j = 1$ and low- x , the integrands asymptote

$$\frac{q_v(x; \mu_0)}{x^{\alpha'_{(-)}t}} \rightarrow \left(\frac{1}{x}\right)^{\alpha_{(-)}(0) + \alpha'_{(-)}t} \quad (32)$$

which is the expected open-string Regge limit, with intercept $\alpha_{(-)}(0)$ and slope $\alpha'_{(-)}$. (28) can be derived holographically [77], however the result is dependent on the choice of the background metric. Here we will fix using the empirical PDFs.

B. Quarks conformal moments: singlet-sea

The holographic parametrization of the conformal moments of the singlet (sea) quark GPDs at $\mu = \mu_0$

is represented by the sum of the sea quark spin- j A-form factor and skewness-dependent spin- j D-form factor as

$$\sum_{q=1}^{N_f} \mathbb{F}_q^{(+)}(j, \eta, t; \mu_0) = \sum_{q=1}^{N_f} \mathcal{F}_q^{(+)}(j, t; \mu_0) + \mathcal{F}_{q\eta}^{(+)}(j, \eta, t; \mu_0), \quad (33)$$

for even $j = 2, 4, \dots$, where we have defined

$$\sum_{q=1}^{N_f} \mathcal{F}_q^{(+)}(j, t; \mu_0) = \int_0^1 dx \sum_{q=1}^{N_f} \frac{q^{(+)}(x; \mu_0)}{x^{1-j+\alpha'_{(+)}t}}, \quad (34)$$

with the input singlet quark PDF

$$\begin{aligned} \sum_{q=1}^{N_f} q^{(+)}(x; \mu_0) &= \sum_{q=1}^{N_f} q(x; \mu_0) + \bar{q}(x; \mu_0) \\ &= \sum_{q=1}^{N_f} H_q^{(+)}(x, \eta = 0, t = 0; \mu_0) \end{aligned} \quad (35)$$

$$\hat{d}_j(\eta, t) - 1 = \eta^j \times \left[\frac{\binom{1-j}{2} j/2}{\binom{1}{2} - j} \times \left(\frac{4m_N^2}{t} \right)^{j/2} \right] + \sum_{n=1}^{(j-2)/2} \eta^{2n} \times \left[\binom{j/2}{n} \frac{\binom{1-j}{2} n}{\binom{1}{2} - j} \times \left(\frac{4m_N^2}{t} \right)^n \right].$$

Here $\binom{m}{n}$ is the Binomial coefficient, and $(q)_n = q(q+1)\dots(q+n-1)$ for $n > 0$ with $(q)_0 = 1$ is the (rising) Pochhammer symbol. Note that the spin-2 A-form factor of the quark gravitational form factor of the proton is given by

$$\sum_{q=1}^{N_f} A_q(t; \mu_0) = \sum_{q=1}^{N_f} \mathcal{F}_q^{(+)}(j = 2, t; \mu_0)$$

and the D-form factor (or the D-term) of the quark gravitational form factor of the proton is given by

$$\eta^2 \sum_{q=1}^{N_f} D_q(t; \mu_0) = \sum_{q=1}^{N_f} \mathcal{F}_{q\eta}^{(+)}(j = 2, \eta, t; \mu_0). \quad (39)$$

C. Gluon conformal moments

The holographic parametrization of the conformal moments of the gluon GPD at finite skewness, and at

at $\mu = \mu_0$. The skewness or η -dependent spin- j D-form factor is given by

$$\begin{aligned} \sum_{q=1}^{N_f} \mathcal{F}_{q\eta}^{(+)}(j, \eta, t; \mu_0) &= \left(\hat{d}_j(\eta, t) - 1 \right) \\ &\times \left[\sum_{q=1}^{N_f} \mathcal{F}_q^{(+)}(j, t; \mu_0) - \mathcal{F}_{q,s}^{(+)}(j, t; \mu_0) \right], \end{aligned} \quad (36)$$

where

$$\sum_{q=1}^{N_f} \mathcal{F}_{q,s}^{(+)}(j, t; \mu_0) \equiv \sum_{q=1}^{N_f} \mathcal{F}_q^{(+)}(j, t; \mu_0, \alpha'_{(+)} \rightarrow \alpha'_{(+),s}), \quad (37)$$

and

$$\begin{aligned} \hat{d}_j(\eta, t) - 1 &= \\ &{}_2F_1 \left(-\frac{j}{2}, -\frac{j-1}{2}; \frac{1}{2} - j; \frac{4m_N^2}{-t} \times \eta^2 \right) - 1. \end{aligned} \quad (38)$$

For even integer $j = 2, 4, \dots$, we can also rewrite (38) as a finite series (or polynomial) in η as

input scale $\mu = \mu_0$ is represented by the sum of the gluon spin- j A-form factor and skewness-dependent spin- j D-form factor as

$$\mathbb{F}_g^{(+)}(j, \eta, t; \mu_0) = \mathcal{A}_g(j, t; \mu_0) + \mathcal{D}_{g\eta}(j, \eta, t; \mu_0), \quad (40)$$

for even $j = 2, 4, \dots$, where we have defined

$$\mathcal{A}_g(j, t; \mu_0) = \int_0^1 dx \frac{xg(x; \mu_0)}{x^{2-j+\alpha'_T t}}. \quad (41)$$

Again we note that for $j = 2$ and low- x , the integrand asymptotes

$$\frac{xg(x; \mu_0)}{x^{\alpha'_T t}} \rightarrow \left(\frac{1}{x} \right)^{\alpha_T(0) + \alpha'_T t} \quad (42)$$

which is the expected closed-string Regge limit, with intercept $\alpha_T(0)$ and slope $\alpha'_T(0)$. Although (41) can be derived holographically [77], here we choose to fix it using the empirical PDFs.

The skewness or η -dependent terms \mathcal{D}_η are given by

$$\mathcal{D}_{g\eta}(j, \eta, t; \mu_0) = \left(\hat{d}_j(\eta, t) - 1 \right) \times [\mathcal{A}_g(j, t; \mu_0) - \mathcal{A}_{gS}(j, t; \mu_0)], \quad (43)$$

where

$$\mathcal{A}_{gS}(j, t; \mu_0) \equiv \mathcal{A}_g(j, t; \mu_0, \alpha'_T \rightarrow \alpha'_S), \quad (44)$$

with the Regge slope parameter α'_S to be fixed by the gluon gravitational form factor of the proton, and $\hat{d}_j(\eta, t)$ — given by (38) or its finite series expansion (39), for even integer $j = 2, 4, \dots$. Note that the spin-2 A-form factor of the gluonic gravitational form factor of the proton is given by [77]

$$\mathcal{A}_g(t; \mu_0) = \mathcal{A}_g(j = 2, t; \mu_0) \quad (45)$$

and the D-form factor (or the D-term) of the gluonic gravitational form factor of the proton is given by

$$\eta^2 D_g(t; \mu_0) = \mathcal{D}_{g\eta}(j = 2, \eta, t; \mu_0).$$

We would like to highlight recent findings from the $J/\Psi - 007$ collaboration at JLab [79]. This collaboration employed the holographic scattering amplitude for near-threshold J/Ψ production by us [80, 81], which correlates with the spin-2 moment $\mathbb{F}_g^{(+)}(2, \eta, t; \mu_0)$ as defined in (40). Through their experiments, they successfully extracted the gluonic spin-2 moment, which show strong agreement with results from lattice QCD [82, 83]. This supports our holographic ansatz for the conformal moments as outlined in (40), establishing a robust experimental and theoretical foundation.

D. Evolution of conformal moments

The leading-order evolution of the conformal moments for valence (non-singlet) quark GPDs is given as follows [77]

$$\mathbb{F}_q^{(-)}(j, \eta, t; \mu) = \mathbb{F}_q^{(-)}(j, \eta, t; \mu_0) \left(\frac{\alpha_s(\mu_0^2)}{\alpha_s(\mu^2)} \right)^{\frac{\gamma_{j-1}^{qq;NS}}{\beta_0}}. \quad (46)$$

Here, $\gamma_j^{qq;NS} \equiv \gamma_{(0)j}^{qq;V;NS}$ denotes the leading-order (LO) vector non-singlet anomalous dimensions:

$$\gamma_j^{qq;NS} = -C_F \left(-4\psi(j+2) + 4\psi(1) + \frac{2}{(j+1)(j+2)} + 3 \right), \quad (47)$$

with $\psi(z)$ representing the digamma function and $\gamma_E = -\psi(1) \approx 0.577216$.

Note that the non-singlet isovector conformal moments are evolved as

$$\mathbb{F}_{u-d}^{(-)}(j, \eta, t; \mu) = \mathbb{F}_{u-d}^{(-)}(j, \eta, t; \mu_0) \left(\frac{\alpha_s(\mu_0^2)}{\alpha_s(\mu^2)} \right)^{\frac{\gamma_{j-1}^{qq;NS}}{\beta_0}}. \quad (48)$$

The evolution equations for the singlet quark and symmetric gluon GPD conformal moments are provided by [77]

$$\begin{aligned} \sum_{q=1}^{N_f} \mathbb{F}_q^{(+)}(j, \eta, t; \mu) &= \left(\frac{\gamma_{j-1}^{qq}}{\gamma_{j-1}^+ - \gamma_{j-1}^-} \right) \\ &\times \left[\Gamma_{j-1}^- \mathbb{F}_j^+(j, \eta, t; \mu_0) \left(\frac{\alpha_s(\mu_0^2)}{\alpha_s(\mu^2)} \right)^{\frac{\gamma_{j-1}^+}{\beta_0}} \right. \\ &\left. - \Gamma_{j-1}^+ \mathbb{F}_j^-(j, \eta, t; \mu_0) \left(\frac{\alpha_s(\mu_0^2)}{\alpha_s(\mu^2)} \right)^{\frac{\gamma_{j-1}^-}{\beta_0}} \right], \quad (49) \end{aligned}$$

$$\begin{aligned} \mathbb{F}_g^{(+)}(j, \eta, t; \mu) &= \left(\frac{\frac{6}{j} \gamma_{j-1}^{gg}}{\gamma_{j-1}^+ - \gamma_{j-1}^-} \right) \\ &\times \left[\mathbb{F}_j^+(j, \eta, t; \mu_0) \left(\frac{\alpha_s(\mu_0^2)}{\alpha_s(\mu^2)} \right)^{\frac{\gamma_{j-1}^+}{\beta_0}} \right. \\ &\left. - \mathbb{F}_j^-(j, \eta, t; \mu_0) \left(\frac{\alpha_s(\mu_0^2)}{\alpha_s(\mu^2)} \right)^{\frac{\gamma_{j-1}^-}{\beta_0}} \right], \quad (50) \end{aligned}$$

where $\Gamma_j^\pm \equiv 1 - \frac{\gamma_j^\pm}{\gamma_j^{qq}}$,

$$\begin{aligned} \mathbb{F}_j^\pm(j, \eta, t; \mu) &= \sum_{q=1}^{N_f} \mathbb{F}_q^{(+)}(j, \eta, t; \mu_0) \\ &+ \left(\frac{\frac{j}{6} \gamma_{j-1}^{gg}}{\gamma_{j-1}^{qq} - \gamma_{j-1}^{\mp}} \right) \mathbb{F}_g^{(+)}(j, \eta, t; \mu_0), \quad (51) \end{aligned}$$

and the eigenvalues γ_j^\pm are defined as:

$$\gamma_j^\pm = \frac{1}{2} \left(\gamma_j^{qq} + \gamma_j^{gg} \pm \sqrt{(\gamma_j^{qq} - \gamma_j^{gg})^2 + 4\gamma_j^{gg}\gamma_j^{qq}} \right). \quad (52)$$

The leading-order (LO) vector singlet anomalous dimensions $\gamma_j^{ab} \equiv \gamma_{(0)j}^{ab;V}$ (with $a = q, g$ and $b = q, g$) are given in [77] (see Eqs.K.31-38), for both the axial-vector (A) and vector (V) ones. Here we need the vector (V) ones.

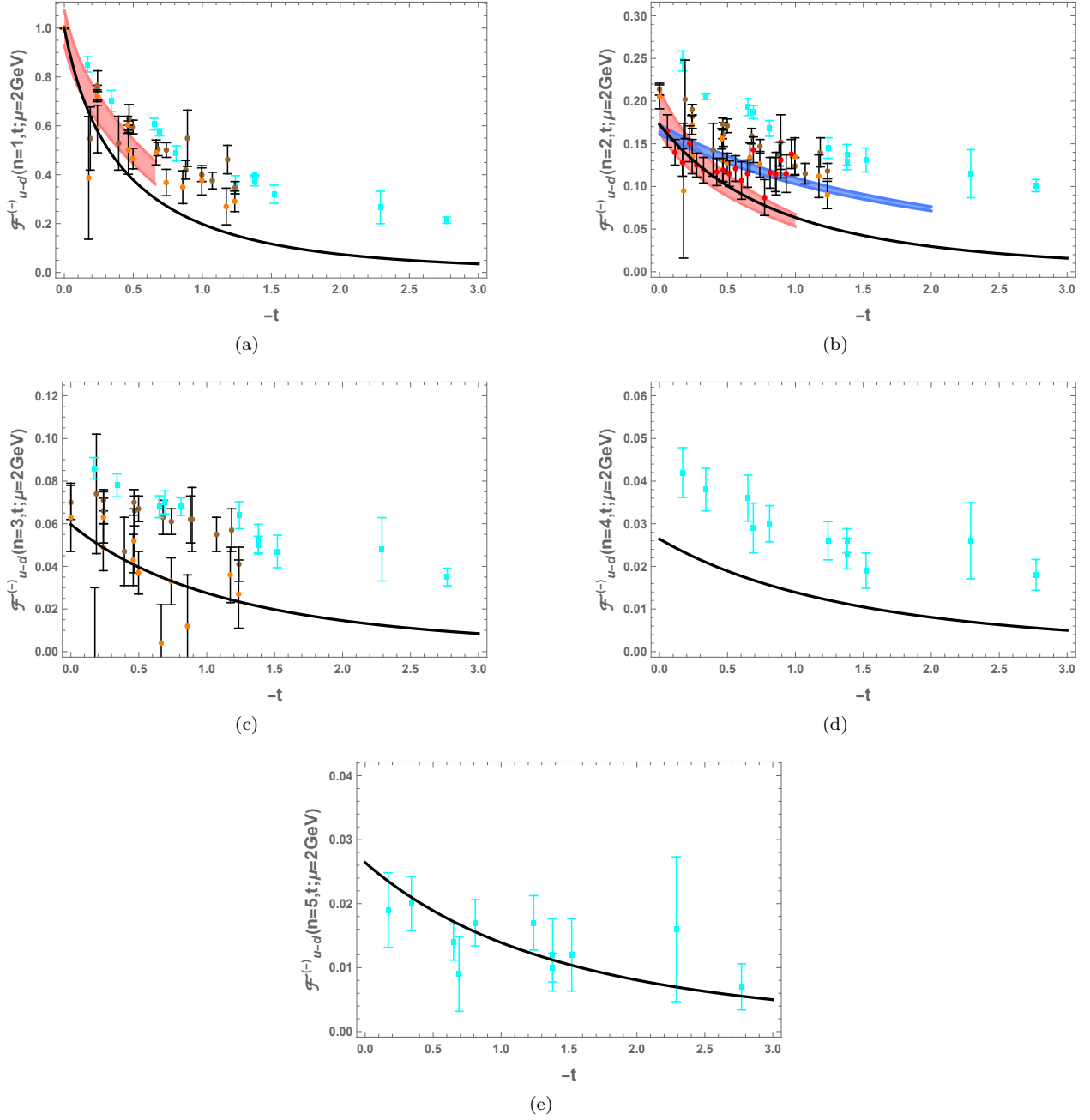


FIG. 1: Our evolved moments of $u - d$ quark GPD $H^{u-d}(x, \eta, t; \mu)$ at $\mu = 2 \text{ GeV}$ (black-solid line). The other colored curves and data points are lattice results from [84] (Cyan data points), [85] (Orange and Brown data points), [19] (Pink curve), [86] (Red data points), and [83] (Blue curve) are shown for comparison.

IV. RESULTS

To proceed, we need to fix the initial quark and gluon conformal moments in (28,34,41). Since the holographic predictions for these moments rely on the choice of the bulk metric, we suggest to use the

empirical quark and gluon PDFs at the lowest resolution point $\mu = \mu_0$, for a model independent initial assessment. In addition, the quark and gluon Regge slopes $\alpha'_{u\pm d, T}$ will be treated as free parameters, to be fixed empirically.

More specifically, we will use the leading-order

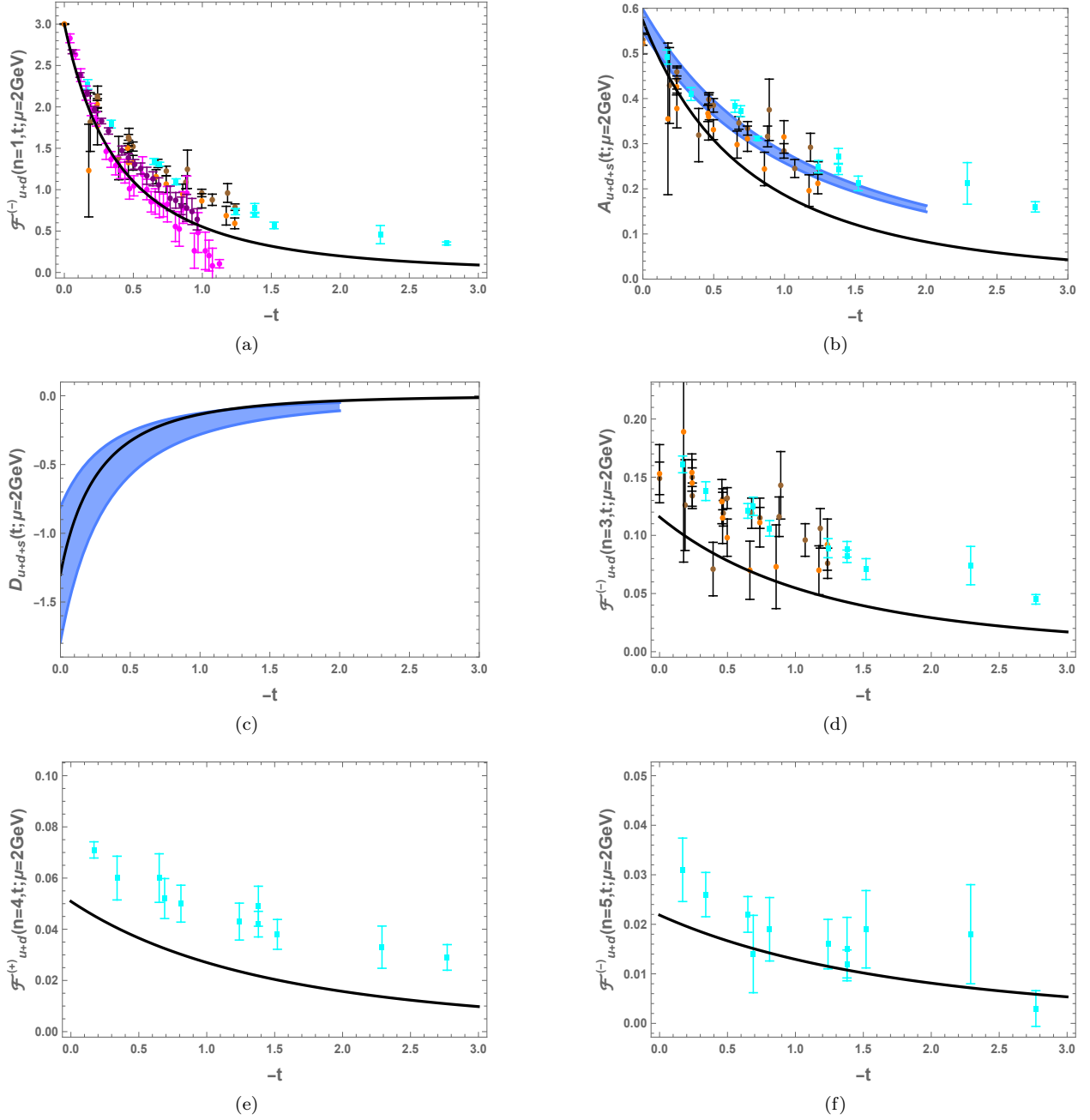


FIG. 2: Our evolved moments of $u + d$ quark GPD $H^{u+d}(x, \eta, t; \mu)$ at $\mu = 2$ GeV (black-solid line). The other colored Conformal Regge theory are lattice results from [84] (Cyan data points), [85] (Orange and brown data points), [87] (Purple data points), [88] (Magenta data points), and [83] (Blue curve) are shown for comparison.

Martin-Stirling-Thorne-Watt (MSTW) 2008 PDF sets [89] at $\mu_0 = 1$ GeV, as quoted in Appendix A for completeness. Their pertinent evolutions to higher resolution say $\mu = 2$ GeV, are summarized in subsection III D. Although the Regge slopes are free parameters fixed empirically, the canonical string val-

ues are $\alpha'_q = (\alpha'_{u+d} + \alpha'_{u-d})/2 \approx 2\alpha'_T = 2\alpha'_g \approx 1 \text{ GeV}^{-2}$ for comparison.

Our study leverages the holographic parametrization, relying on only the quark and gluon empirical Regge slope parameters, listed in Table I, $\alpha'_{u\pm d}$ (including $\alpha'_{(+,s)}$) and $\alpha'_{T,S}$ are fixed by the electromag-

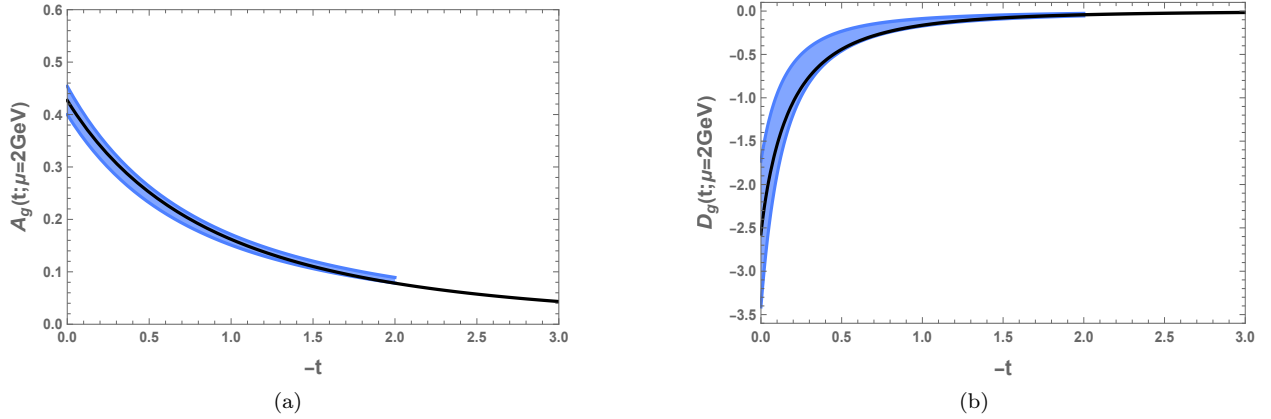


FIG. 3: Our evolved moments of the symmetric gluon GPD $H_g^{(+)}(x, \eta, t; \mu)$ at $\mu = 2$ GeV, are represented by black line. The blue curve corresponding to lattice data from [83] is shown for comparison.

netic and gravitational form factors of the proton. We note that the empirical quark and gluon Regge intercepts fixed by the global fits, are consistent with the canonical string values.

We now proceed to compare in details our results for the holographically parametrized GPDs, with the recently reported lattice nucleon quark GPDs, both for the lowest moments and also the full quark GPDs at finite skewness.

A. Moments versus lattice

In Fig. 1, we compare our evolved lowest moments $n = 1, 2, \dots, 5$ for the nucleon valence $u - d$ (isovector) quark GPD $H^{u-d}(x, \eta, t; \mu) \equiv H_{u-d}^{(-)}(x, \eta, t; \mu)$ at $\mu = 2$ GeV, to the recently reported lattice data. Our results are represented by the black-solid lines. The lattice results from different collaborations are shown as data points or colored spreads. The lattice results are from [84] (Cyan data points), [85] (Orange and Brown data points), [19] (Pink curve), [86] (Red data points), and [83] (Blue curve). Overall, our results are in relative good agreement with the reported lattice results.

In Fig. 2 we compare our evolved lowest moments for the nucleon sea $u + d$ quark GPD $H^{u+d}(x, \eta, t; \mu)$ at $\mu = 2$ GeV, to the lattice results. Again, our results are represented by the black-solid lines. The lattice results from different collaborations are shown as data points or colored spreads. They are from [84] (Cyan data points), [85] (Orange and Brown data points), [87] (Purple data points), [88] (Magenta data points), and [83] (Blue curve) are shown for comparison. Again, the agreement with the reported lattice results, is relatively good.

In Fig. 3 we compare our evolved and symmetric gluon GPD $H_g^{(+)}(x, \eta, t; \mu)$ at $\mu = 2$ GeV, to the lattice results reported in [83]. Our results are represented by the black-solid line, and the lattice results by the blue-spread. The agreement of the holographic results with the lattice results is good.

B. GPDs versus lattice

In Fig. 4a we show our full GPDs for the nucleon valence $u - d$ (isovector) quark GPD $H^{u-d}(x, \eta, t; \mu)$ of (12) using the conformal moments (29), for different values of the skewness η and Mandelstam t . The colored curves refer to different kinematics with Purple for $\eta = 0$, $-t = 0$, and $\mu = 2$ GeV, Green for $\eta = 1/3$, $-t = 0.69$ GeV², and $\mu = 2$ GeV, Yellow for $\eta = 0.1$, $-t = 0.23$ GeV², and $\mu = 2$ GeV, and Pink for $\eta = 0$, $-t = 0.39$ GeV², and $\mu = 3$ GeV. In Fig. 4b the corresponding lattice results with colored curves are shown for comparison. The lattice results are from [21] (Purple, and Green curves), [90] (Yellow curve), and [19] (Pink curve) are shown with matching color coding for direct comparison.

In Fig. 5, we show a one-to-one comparison of our results in black-solid lines, for the nucleon valence $u - d$ quark GPD $H^{u-d}(x, \eta, t; \mu)$, for different kinematics. The colored curves are the lattice data from [21] (Purple, Cyan, and Green curves), from [90] (Blue curve), and from [19] (Pink curve) with

- a: $\eta = 0$, $-t = 0$, and $\mu = 2$ GeV;
- b: $\eta = 0$, $-t = 0.69$ GeV², and $\mu = 2$ GeV;
- c: $\eta = 0$, $-t = 0.39$ GeV², and $\mu = 3$ GeV;
- d: $\eta = 1/3$, $-t = 0.69$ GeV², and $\mu = 2$ GeV;
- e: $\eta = 0.1$, $-t = 0.23$ GeV², and $\mu = 2$ GeV.

The overall agreement with the reported lattice re-

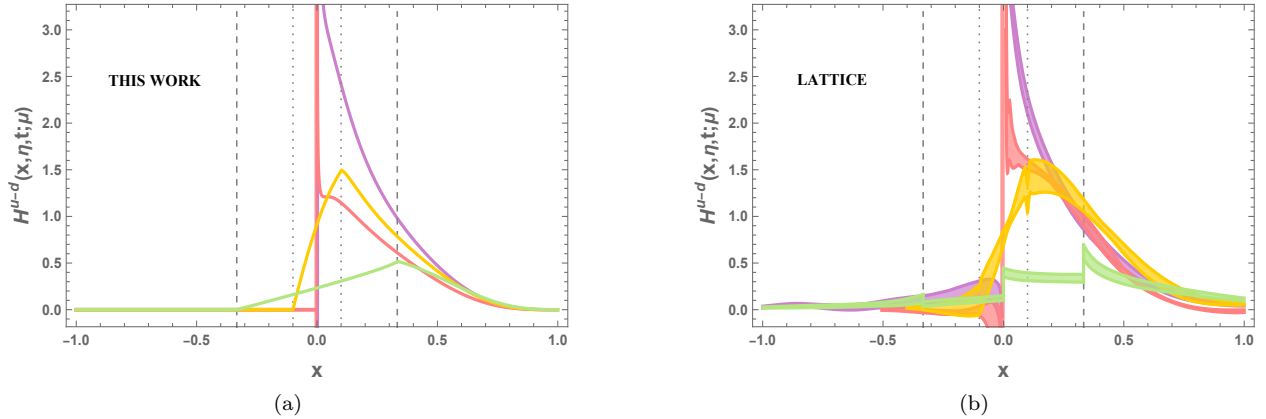


FIG. 4: (a) The colored solid curves represent our numerical results for the $u-d$ (isovector) quark GPD $H^{u-d}(x, \eta, t; \mu)$ of (12) using the conformal moments (29), interpolated from our numerical data. The curves correspond to various kinematic configurations: purple for $\eta = 0$, $-t = 0$, and $\mu = 2$ GeV, green for $\eta = 1/3$, $-t = 0.69$ GeV², and $\mu = 2$ GeV, yellow for $\eta = 0.1$, $-t = 0.23$ GeV², and $\mu = 2$ GeV, and pink for $\eta = 0$, $-t = 0.39$ GeV², and $\mu = 3$ GeV. (b) Corresponding lattice results from [21] (purple, and green curves), [90] (yellow curve), and [19] (pink curve) are shown with matching color coding for direct comparison.

sults at different kinematical regimes, is again good.

C. Gluon, valence and sea quark GPDs

In Fig. 7a we show our prediction for the gluon GPD $H_g^{(+)}(x, \eta, t; \mu)$, as defined in (26). The prediction follows from the gluon conformal moments from (40), based on the MSTW2008lo gluon PDF from [89]. Our explicit results are shown in open circles with numerical interpolation for different kinematics $\eta = 0, -t = 0$ (purple curve), $\eta = 0.1, -t = 0.23$ GeV² (yellow curve) and $\eta = 1/3, -t = 0.69$ GeV² at the evolved resolution $\mu = 2$ GeV.

In Fig. 7b, we show our predictions for the singlet (sea) quark GPD $H_{u+d+s}^{(+)}(x, \eta, t; \mu)$, following from (15). The results follow from the singlet quark conformal moments in (33) and the MSTW2008lo singlet (sea) quark PDF in [89]. In addition, we use the Regge slope parameters $\alpha'_{(+)} = \alpha'_{u+d}$, and $\alpha'_{(+),s}$ listed in Table I. The curve color display and kinematics is the same as that in Fig. 7a.

For the non-singlet (valence) quark GPDs,

Figs. 7c-7d show our predictions for $H_{u,d}^{(-)}(x, \eta, t; \mu)$, as in (9). The results follow from the non-singlet quark conformal moments given in (27), using the MSTW2008lo non-singlet (valence) quark PDF [89]. The curve color display and kinematics is the same as that in Fig. 7a.

D. Flavor separated quark GPDs

In Fig. 6 we show our predictions for the flavor separated nucleon u, d quark GPDs $H^{u,d}(x, \eta, t; \mu)$. For the flavor separation, we have ignored the strange quark contribution and assumed $H_{u+d+s}^{(+)} \approx H_{u+d}^{(+)}$. The flavor separated GPDs reduce to the expected u, d PDFs at $\eta = t = 0$ with the expected differences (Purple curves). The differences are less pronounced for the u, d GPDs at $\eta = 1, 3, -t = 0.69$ GeV² (Green curves) and $\eta = 0.1, -t = 0.23$ GeV² (Yellow curves). For the flavor (up (u) quark and down (d) quark) separation, as well as for separation into quark and anti-quark (in the positive (+x), and negative (-x) regions of quark GPDs, respectively), we made use of the following relations

$$H^{u+d}(+x, \eta, t; \mu) = \frac{1}{2} \left(H_{u+d}^{(-)}(x, \eta, t; \mu) + H_{u+d}^{(+)}(x, \eta, t; \mu) \right), \quad (53)$$

$$H^{u+d}(-x, \eta, t; \mu) = \frac{1}{2} \left(H_{u+d}^{(-)}(x, \eta, t; \mu) - H_{u+d}^{(+)}(x, \eta, t; \mu) \right), \quad (54)$$

$$H^u(+x, \eta, t; \mu) = \frac{1}{2} \left(H^{u+d}(+x, \eta, t; \mu) + H^{u-d}(+x, \eta, t; \mu) \right), \quad (55)$$

$$H^u(-x, \eta, t; \mu) = \frac{1}{2} \left(H^{u+d}(-x, \eta, t; \mu) + H^{u-d}(-x, \eta, t; \mu) \right), \quad (56)$$

$$H^d(+x, \eta, t; \mu) = \frac{1}{2} \left(H^{u+d}(+x, \eta, t; \mu) - H^{u-d}(+x, \eta, t; \mu) \right), \quad (57)$$

$$H^d(-x, \eta, t; \mu) = \frac{1}{2} \left(H^{u+d}(-x, \eta, t; \mu) - H^{u-d}(-x, \eta, t; \mu) \right). \quad (58)$$

TABLE I: Regge slope parameters for the holographic parametrization of conformal moments.

Parameter	Value (GeV ⁻²)
α'_T	0.627
α'_S	4.277
$\alpha'_{(+)} = \alpha'_{(-)} = \alpha'_{u+d}$	0.891
α'_{u-d}	1.069
$\alpha'_{(+),s}$	1.828

V. CONCLUSIONS

The string-based parametrization we have presented, shows how to extend our recent proposal for the nucleon GPDs [77] from the ERL regime at low-x, to the DGLAP regime at large-x. More specifically, the GPDs are expanded in terms of integer valued conformal moments, using an ortho-complete basis set of conformal PWs. Using the Sommerfeld-Watson transform, the series is then analytically continued in the complex j-plane, with a pertinent analytical continuation of the PWs whatever the skewness. This proposal is general, and holds for any dynamical perturbative or non-perturbative analysis of the GPDs.

The spin-j conformal moments in the integral transform, encode the essential hadronic content of the GPDs. In the gravity dual approach at large skewness and small parton-x, they are described by Reggeized exchanges of bulk spin-j mesons (open string Regge) or spin-j glueballs (closed string Regge). These exchanges are captured by generalized string based form factors through pertinent confluent hypergeometric functions [77], with only the Regge intercepts and slopes as parameters. Analyticity as enforced by the integral transforms, allows for the string based result to be used as parametrizations of the spin-j conformal moments for any skewness.

At zero skewness, the spin-j conformal moments are moments of the pertinent quark and gluon parton distribution functions. At low resolution, we have elected to fix these spin-j conformal moments using the empirical MSTW PDFs, since the gravity dual description of the PDFs is mostly limited to the Regge regime. Their evolution to higher resolution follows from general QCD evolution, as they are form invariant. Overall, our results for the string based parametrization of the GPDs for the moments of the nucleon singlet and non-singlet quark GPDs are in fair agreement with those reported by various lattice collaborations. We expect more precise results with physical quark masses from lattice will be in better agreement with our moments. Also our results for the nucleon isovector quark GPDs at different kinematics with zero and finite skewness, are in good agreement with most of the lattice results reported recently. More importantly, we have used the string based parametrization to predict the nucleon gluon, valence and sea quark GPDs, which are yet to be accessed by current lattice simulations. The extension of our analysis to the polarized, and helicity flip nucleon GPDs, as well as other hadrons will be addressed in upcoming publications.

In sum, the string based parametrization of the quark and gluon GPDs we have presented, obey all the constraints required by symmetry and analyticity. Their explicit form should prove useful for the program of global GPDs data analyses, bypassing the de-convolution problem, to be carried out by the quark-gluon-tomography (QGT) collaboration. Most importantly, they should also be useful for the analysis of a number of exclusive processes currently carried out at JLab, and planned for the upcoming EIC.

Acknowledgments

K.M. is supported by U.S. DOE Grant No. DE-

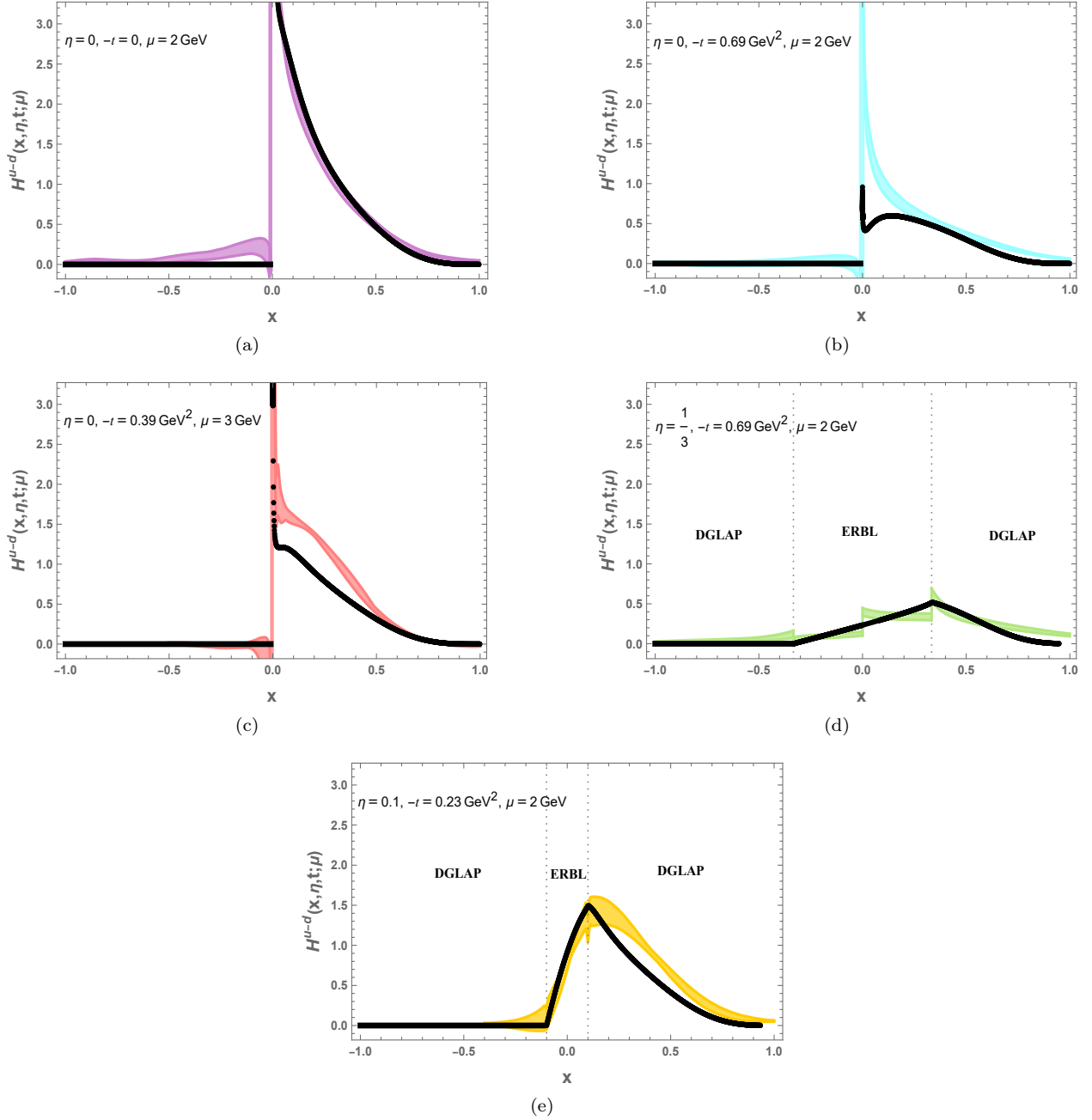


FIG. 5: Our numerical results, for the $u-d$ (isovector) quark GPD $H^{u-d}(x, \eta, t; \mu)$, are represented by black data points. The other colored curves, corresponding to lattice data, from [21] (Purple, Cyan, and Green curves), [90] (Blue curve), and [19] (Pink curve) are shown for comparison. The figures illustrate various kinematic scenarios: (a) $\eta = 0, -t = 0$, and $\mu = 2 \text{ GeV}$ (b) $\eta = 0, -t = 0.69 \text{ GeV}^2$, and $\mu = 2 \text{ GeV}$ (c) $\eta = 0, -t = 0.39 \text{ GeV}^2$, and $\mu = 3 \text{ GeV}$, (d) $\eta = 1/3, -t = 0.69 \text{ GeV}^2$, and $\mu = 2 \text{ GeV}$ (e) $\eta = 0.1, -t = 0.23 \text{ GeV}^2$, and $\mu = 2 \text{ GeV}$.

FG02-04ER41302, and thanks Konstantinos Orginos and Christian Weiss for discussions and hospitality at JLab where part of this work was carried out. I.Z. is supported by the U.S. DOE Grant No. DE-FG-

88ER40388. This research is also supported in part within the framework of the Quark-Gluon Tomography (QGT) Topical Collaboration, under contract no. DE-SC0023646.

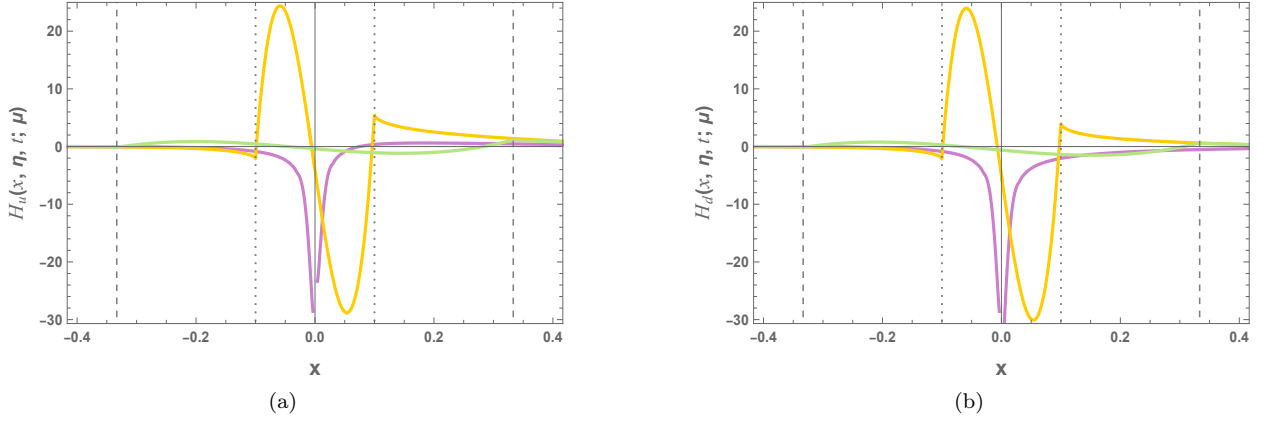


FIG. 6: The colored solid curves represent our numerical results for the flavor separated u and d quark GPDs $H^{u,d}(x, \eta, t; \mu)$, interpolated from our numerical data. The curves refer to various kinematics: Purple for $\eta = 0$, $-t = 0$, and $\mu = 2$ GeV, Green for $\eta = 1/3$, $-t = 0.69$ GeV², and $\mu = 2$ GeV, and Yellow for $\eta = 0.1$, $-t = 0.23$ GeV², and $\mu = 2$ GeV.

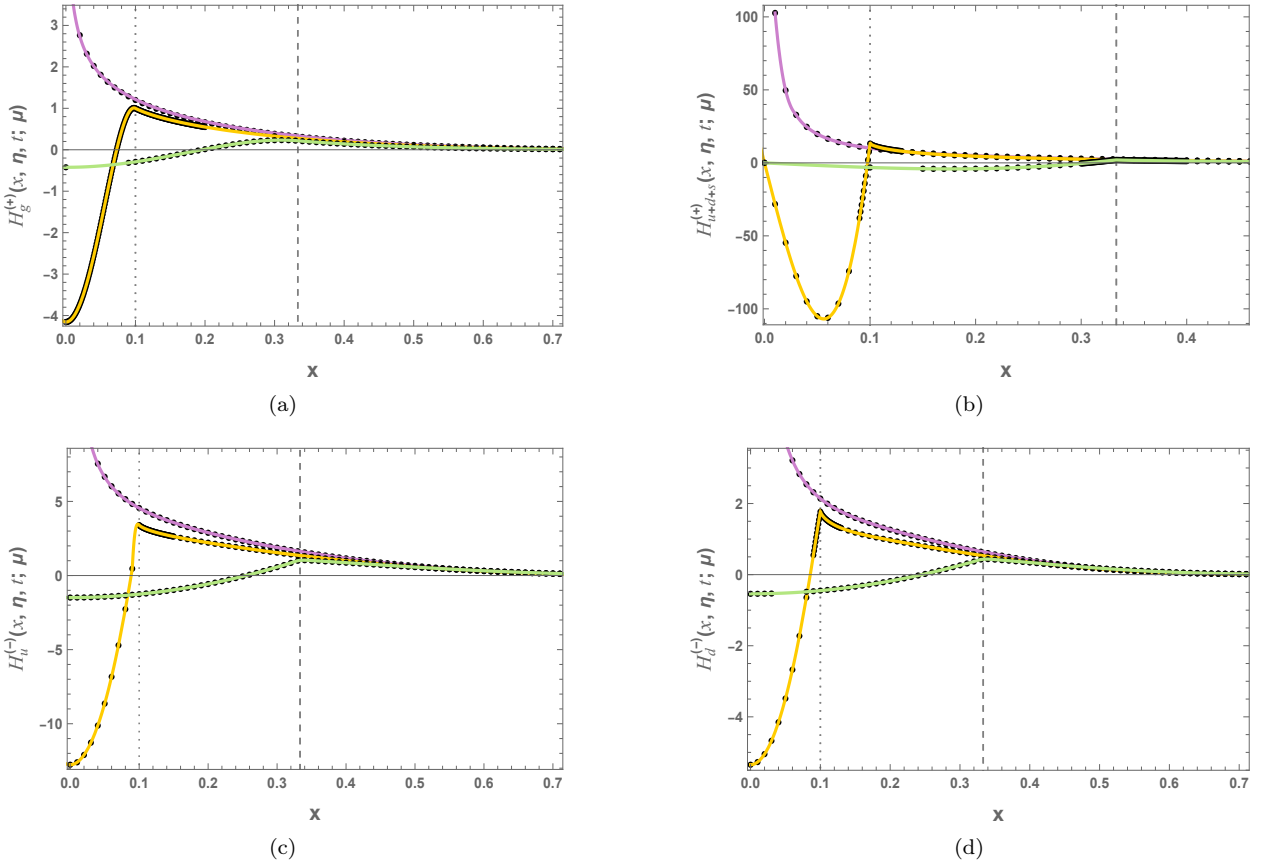


FIG. 7: Our numerical results for the gluon GPD (a), sea quark GPD (b), valence up quark GPD (c), and valence down quark GPD (d) are represented by black data points. The colored curves are our interpolation of the numerical data. The figures illustrate various kinematic scenarios: (Purple curves) $\eta = 0$, $-t = 0$, and $\mu = 2$ GeV, (Yellow curves) $\eta = 0.1$, $-t = 0.23$ GeV², and $\mu = 2$ GeV, (Green curves) $\eta = 1/3$, $-t = 0.69$ GeV². All curves are evolved to the resolution $\mu = 2$ GeV.

Appendix A: MSTW PDFs

To fix the input conformal moments of the quark and gluon GPDs at low resolution $\mu = \mu_0$, we will use the empirical nucleon quark and gluon PDFs,

instead of the holographic PDFs which depend on the choice of the bulk metric, and hence model dependent. More specifically, we will use the leading-order Martin-Stirling-Thorne-Watt (MSTW) 2008 PDF sets [89] at $\mu_0 = 1$ GeV

$$\begin{aligned}
u_v(x; \mu_0) &\equiv u(x; \mu_0) - \bar{u}(x; \mu_0) = 1.4335 x^{-0.54768} (1-x)^{3.0409} (8.9924x - 2.3737\sqrt{x} + 1), \\
d_v(x; \mu_0) &\equiv d(x; \mu_0) - \bar{d}(x; \mu_0) = 5.0903 x^{-0.28022} (1-x)^{5.1244} (7.473x - 4.3654\sqrt{x} + 1), \\
s_v(x; \mu_0) &\equiv s(x; \mu_0) - \bar{s}(x; \mu_0) = 0.011523 x^{-1.299} (1-x)^{10.285} \left(\frac{x}{0.017414} - 1 \right), \\
\Delta(x; \mu_0) &\equiv \bar{d}(x; \mu_0) - \bar{u}(x; \mu_0) = 8.9413 x^{0.876} (1-x)^{10.8801} (-36.507x^2 + 8.4703x + 1), \\
s^{(+)}(x; \mu_0) &\equiv s(x; \mu_0) + \bar{s}(x; \mu_0) = 0.10302 x^{-1.16276} (1-x)^{13.242} (16.865x - 2.9012\sqrt{x} + 1), \\
xg(x; \mu_0) &= 0.0012216 x^{-0.83657} (1-x)^{2.3882} (1445.5x - 38.997\sqrt{x} + 1) \quad (A1)
\end{aligned}$$

and

$$\begin{aligned}
S(x; \mu_0) &\equiv 2(\bar{u}(x; \mu_0) + \bar{d}(x; \mu_0)) + s(x; \mu_0) + \bar{s}(x; \mu_0) \\
&= 0.59964 x^{-1.16276} (1-x)^{8.8801} (16.865x - 2.9012\sqrt{x} + 1). \quad (A2)
\end{aligned}$$

We note that in our numerical evaluation of the sea and $u - d$ (isovector) quark GPDs, we used

$$\sum_{q=1}^{N_f=3} H_q^{(+)}(x, \eta = 0, t = 0; \mu_0) = \sum_{q=1}^{N_f=3} q(x; \mu_0) + \bar{q}(x; \mu_0) = u_v(x; \mu_0) + d_v(x; \mu_0) + S(x; \mu_0), \quad (A3)$$

and

$$H^{u-d}(x, \eta, t; \mu_0) \approx u_v(x; \mu_0) - d_v(x; \mu_0), \quad (A4)$$

respectively, with $\Delta(x; \mu_0) = \bar{d}(x; \mu_0) - \bar{u}(x; \mu_0) \approx 0$.

-
- | | |
|--|---|
| <p>[1] C. G. Callan, Jr. and D. J. Gross, <i>Phys. Rev. Lett.</i> 22, 156 (1969).</p> <p>[2] D. J. Gross and F. Wilczek, <i>Phys. Rev. Lett.</i> 30, 1343 (1973).</p> <p>[3] H. D. Politzer, <i>Phys. Rev. Lett.</i> 30, 1346 (1973).</p> <p>[4] J. C. Collins, D. E. Soper, and G. F. Sterman, <i>Adv. Ser. Direct. High Energy Phys.</i> 5, 1 (1989), arXiv:hep-ph/0409313.</p> <p>[5] J. Collins, <i>Foundations of Perturbative QCD</i>, Cambridge Monographs on Particle Physics, Nuclear Physics and Cosmology, Vol. 32 (Cambridge University Press, 2023).</p> <p>[6] D. Müller, D. Robaschik, B. Geyer, F. M. Dittes, and J. Hořejši, <i>Fortsch. Phys.</i> 42, 101 (1994), arXiv:hep-ph/9812448.</p> <p>[7] A. V. Radyushkin, <i>Phys. Lett. B</i> 380, 417 (1996), arXiv:hep-ph/9604317.</p> <p>[8] A. V. Radyushkin, <i>Phys. Lett. B</i> 385, 333 (1996), arXiv:hep-ph/9605431.</p> | <p>[9] X.-D. Ji, <i>Phys. Rev. D</i> 55, 7114 (1997), arXiv:hep-ph/9609381.</p> <p>[10] A. V. Radyushkin, <i>Phys. Rev. D</i> 56, 5524 (1997), arXiv:hep-ph/9704207.</p> <p>[11] X.-D. Ji, <i>J. Phys. G</i> 24, 1181 (1998), arXiv:hep-ph/9807358.</p> <p>[12] K. Goeke, M. V. Polyakov, and M. Vanderhaeghen, <i>Prog. Part. Nucl. Phys.</i> 47, 401 (2001), arXiv:hep-ph/0106012.</p> <p>[13] M. Diehl, <i>Phys. Rept.</i> 388, 41 (2003), arXiv:hep-ph/0307382.</p> <p>[14] A. V. Belitsky and A. V. Radyushkin, <i>Phys. Rept.</i> 418, 1 (2005), arXiv:hep-ph/0504030.</p> <p>[15] C. Mezrag, <i>Few Body Syst.</i> 63, 62 (2022), arXiv:2207.13584 [hep-ph].</p> <p>[16] J.-W. Chen, H.-W. Lin, and J.-H. Zhang, <i>Nucl. Phys. B</i> 952, 114940 (2020), arXiv:1904.12376 [hep-lat].</p> <p>[17] H.-W. Lin, <i>Phys. Lett. B</i> 846, 138181 (2023),</p> |
|--|---|

- arXiv:2310.10579 [hep-lat].
- [18] H.-W. Lin, *Few Body Syst.* **64**, 58 (2023).
- [19] H.-W. Lin, *Phys. Rev. Lett.* **127**, 182001 (2021), arXiv:2008.12474 [hep-ph].
- [20] H.-W. Lin, *Phys. Lett. B* **824**, 136821 (2022), arXiv:2112.07519 [hep-lat].
- [21] C. Alexandrou, K. Cichy, M. Constantinou, K. Hadjiyiannakou, K. Jansen, A. Scapellato, and F. Steffens, *Phys. Rev. Lett.* **125**, 262001 (2020), arXiv:2008.10573 [hep-lat].
- [22] C. Alexandrou, K. Cichy, M. Constantinou, K. Hadjiyiannakou, K. Jansen, A. Scapellato, and F. Steffens, *Phys. Rev. D* **105**, 034501 (2022), arXiv:2108.10789 [hep-lat].
- [23] S. Bhattacharya, K. Cichy, M. Constantinou, J. Dodson, X. Gao, A. Metz, S. Mukherjee, A. Scapellato, F. Steffens, and Y. Zhao, *Phys. Rev. D* **106**, 114512 (2022), arXiv:2209.05373 [hep-lat].
- [24] X. Ji, *Phys. Rev. Lett.* **110**, 262002 (2013), arXiv:1305.1539 [hep-ph].
- [25] X. Ji, *Sci. China Phys. Mech. Astron.* **57**, 1407 (2014), arXiv:1404.6680 [hep-ph].
- [26] X. Ji, Y.-S. Liu, Y. Liu, J.-H. Zhang, and Y. Zhao, *Rev. Mod. Phys.* **93**, 035005 (2021), arXiv:2004.03543 [hep-ph].
- [27] A. V. Radyushkin, *Phys. Rev. D* **96**, 034025 (2017), arXiv:1705.01488 [hep-ph].
- [28] K. Orginos, A. Radyushkin, J. Karpie, and S. Zafeiropoulos, *Phys. Rev. D* **96**, 094503 (2017), arXiv:1706.05373 [hep-ph].
- [29] N. d'Hose, S. Niccolai, and A. Rostomyan, *Eur. Phys. J. A* **52**, 151 (2016).
- [30] M. Guidal, H. Moutarde, and M. Vanderhaeghen, *Rept. Prog. Phys.* **76**, 066202 (2013), arXiv:1303.6600 [hep-ph].
- [31] K. Kumericki, S. Liuti, and H. Moutarde, *Eur. Phys. J. A* **52**, 157 (2016), arXiv:1602.02763 [hep-ph].
- [32] A. Accardi *et al.*, *Eur. Phys. J. A* **52**, 268 (2016), arXiv:1212.1701 [nucl-ex].
- [33] R. Abdul Khalek *et al.*, (2021), arXiv:2103.05419 [physics.ins-det].
- [34] D. P. Anderle *et al.*, (2021), arXiv:2102.09222 [nucl-ex].
- [35] X.-D. Ji, W. Melnitchouk, and X. Song, *Phys. Rev. D* **56**, 5511 (1997), arXiv:hep-ph/9702379.
- [36] I. V. Anikin, D. Binosi, R. Medrano, S. Noguera, and V. Vento, *Eur. Phys. J. A* **14**, 95 (2002), arXiv:hep-ph/0109139.
- [37] S. Scopetta and V. Vento, *Eur. Phys. J. A* **16**, 527 (2003), arXiv:hep-ph/0201265.
- [38] S. Boffi, B. Pasquini, and M. Traini, *Nucl. Phys. B* **649**, 243 (2003), arXiv:hep-ph/0207340.
- [39] S. Scopetta and V. Vento, *Phys. Rev. D* **69**, 094004 (2004), arXiv:hep-ph/0307150.
- [40] V. Y. Petrov, P. V. Pobylitsa, M. V. Polyakov, I. Bornig, K. Goeke, and C. Weiss, *Phys. Rev. D* **57**, 4325 (1998), arXiv:hep-ph/9710270.
- [41] M. Penttinen, M. V. Polyakov, and K. Goeke, *Phys. Rev. D* **62**, 014024 (2000), arXiv:hep-ph/9909489.
- [42] A. Vega, I. Schmidt, T. Gutsche, and V. E. Lyubovitskij, *Phys. Rev. D* **83**, 036001 (2011), arXiv:1010.2815 [hep-ph].
- [43] M. Rinaldi, *Phys. Lett. B* **771**, 563 (2017), arXiv:1703.00348 [hep-ph].
- [44] M. C. Traini, *Eur. Phys. J. C* **77**, 246 (2017), arXiv:1608.08410 [hep-ph].
- [45] G. F. de Teramond, T. Liu, R. S. Sufian, H. G. Dosch, S. J. Brodsky, and A. Deur (HLFHS), *Phys. Rev. Lett.* **120**, 182001 (2018), arXiv:1801.09154 [hep-ph].
- [46] C. Mondal and D. Chakrabarti, *Eur. Phys. J. C* **75**, 261 (2015), arXiv:1501.05489 [hep-ph].
- [47] D. Chakrabarti and C. Mondal, *Phys. Rev. D* **92**, 074012 (2015), arXiv:1509.00598 [hep-ph].
- [48] C. Mondal, *Eur. Phys. J. C* **77**, 640 (2017), arXiv:1709.06877 [hep-ph].
- [49] D. Chakrabarti and C. Mondal, *Phys. Rev. D* **88**, 073006 (2013), arXiv:1307.5128 [hep-ph].
- [50] B. Gurjar, C. Mondal, and D. Chakrabarti, *Phys. Rev. D* **107**, 054013 (2023), arXiv:2209.14285 [hep-ph].
- [51] E. Shuryak and I. Zahed, *Phys. Rev. D* **107**, 094005 (2023), arXiv:2301.12238 [hep-ph].
- [52] Y. Liu, S. Xu, C. Mondal, X. Zhao, and J. P. Vary, (2024), arXiv:2403.05922 [hep-ph].
- [53] A. V. Radyushkin, *Phys. Rev. D* **59**, 014030 (1999), arXiv:hep-ph/9805342.
- [54] A. V. Radyushkin, *Phys. Lett. B* **449**, 81 (1999), arXiv:hep-ph/9810466.
- [55] M. V. Polyakov and C. Weiss, *Phys. Rev. D* **60**, 114017 (1999), arXiv:hep-ph/9902451.
- [56] I. V. Musatov and A. V. Radyushkin, *Phys. Rev. D* **61**, 074027 (2000), arXiv:hep-ph/9905376.
- [57] S. V. Goloskokov and P. Kroll, *Eur. Phys. J. C* **65**, 137 (2010), arXiv:0906.0460 [hep-ph].
- [58] S. V. Goloskokov and P. Kroll, *Eur. Phys. J. C* **42**, 281 (2005), arXiv:hep-ph/0501242.
- [59] S. V. Goloskokov and P. Kroll, *Eur. Phys. J. C* **53**, 367 (2008), arXiv:0708.3569 [hep-ph].
- [60] M. Vanderhaeghen, P. A. M. Guichon, and M. Guidal, *Phys. Rev. Lett.* **80**, 5064 (1998).
- [61] M. Vanderhaeghen, P. A. M. Guichon, and M. Guidal, *Phys. Rev. D* **60**, 094017 (1999), arXiv:hep-ph/9905372.
- [62] M. Guidal, M. V. Polyakov, A. V. Radyushkin, and M. Vanderhaeghen, *Phys. Rev. D* **72**, 054013 (2005), arXiv:hep-ph/0410251.
- [63] M. V. Polyakov, *Nucl. Phys. B* **555**, 231 (1999), arXiv:hep-ph/9809483.
- [64] M. V. Polyakov and A. G. Shuvaev, (2002), arXiv:hep-ph/0207153.
- [65] D. Mueller and A. Schafer, *Nucl. Phys. B* **739**, 1 (2006), arXiv:hep-ph/0509204.
- [66] K. Kumericki, D. Mueller, and K. Passek-Kumericki, *Nucl. Phys. B* **794**, 244 (2008), arXiv:hep-ph/0703179.
- [67] K. Kumericki and D. Mueller, *Nucl. Phys. B* **841**, 1 (2010), arXiv:0904.0458 [hep-ph].
- [68] M. V. Polyakov and K. M. Semenov-Tian-Shansky, *Eur. Phys. J. A* **40**, 181 (2009), arXiv:0811.2901 [hep-ph].

- [69] D. Müller, M. V. Polyakov, and K. M. Semenov-Tian-Shansky, *JHEP* **03**, 052 (2015), [arXiv:1412.4165 \[hep-ph\]](#).
- [70] M. Čuić, *Imaging of the three-dimensional quark-gluon structure of the proton via analysis of deeply virtual electron scattering*, Ph.D. thesis, Zagreb U., Phys. Dept. (2024).
- [71] Y. Guo, X. Ji, and K. Shiells, *JHEP* **09**, 215 (2022), [arXiv:2207.05768 \[hep-ph\]](#).
- [72] Y. Guo, X. Ji, M. G. Santiago, K. Shiells, and J. Yang, *JHEP* **05**, 150 (2023), [arXiv:2302.07279 \[hep-ph\]](#).
- [73] M. Čuić, G. Duplančić, K. Kumerički, and K. Passek-K., *JHEP* **12**, 192 (2023), [Erratum: *JHEP* 02, 225 (2024)], [arXiv:2310.13837 \[hep-ph\]](#).
- [74] A. Hannaford-Gunn, K. U. Can, J. A. Crawford, R. Horsley, P. E. L. Rakow, G. Schierholz, H. Stüben, R. D. Young, and J. M. Zanotti, (2024), [arXiv:2405.06256 \[hep-lat\]](#).
- [75] V. Bertone, H. Dutrioux, C. Mezrag, H. Moutarde, and P. Sznajder, *Phys. Rev. D* **103**, 114019 (2021), [arXiv:2104.03836 \[hep-ph\]](#).
- [76] H. Nastase, *Introduction to the ADS/CFT Correspondence* (Cambridge University Press, 2015).
- [77] K. A. Mamo and I. Zahed, *Phys. Rev. D* **108**, 086026 (2023), [arXiv:2206.03813 \[hep-ph\]](#).
- [78] K. A. Mamo and I. Zahed, *Nucl. Phys. B* **997**, 116388 (2023), [arXiv:2106.00752 \[hep-ph\]](#).
- [79] B. Duran *et al.*, *Nature* **615**, 813 (2023), [arXiv:2207.05212 \[nucl-ex\]](#).
- [80] K. A. Mamo and I. Zahed, *Phys. Rev. D* **101**, 086003 (2020), [arXiv:1910.04707 \[hep-ph\]](#).
- [81] K. A. Mamo and I. Zahed, (2022), [arXiv:2204.08857 \[hep-ph\]](#).
- [82] D. A. Pefkou, D. C. Hackett, and P. E. Shanahan, *Phys. Rev. D* **105**, 054509 (2022), [arXiv:2107.10368 \[hep-lat\]](#).
- [83] D. C. Hackett, D. A. Pefkou, and P. E. Shanahan, (2023), [arXiv:2310.08484 \[hep-lat\]](#).
- [84] S. Bhattacharya, K. Cichy, M. Constantinou, X. Gao, A. Metz, J. Miller, S. Mukherjee, P. Petreczky, F. Steffens, and Y. Zhao, *Phys. Rev. D* **108**, 014507 (2023), [arXiv:2305.11117 \[hep-lat\]](#).
- [85] P. Hagler *et al.* (LHPC), *Phys. Rev. D* **77**, 094502 (2008), [arXiv:0705.4295 \[hep-lat\]](#).
- [86] C. Alexandrou *et al.*, *Phys. Rev. D* **101**, 034519 (2020), [arXiv:1908.10706 \[hep-lat\]](#).
- [87] C. Alexandrou, S. Bacchio, M. Constantinou, J. Finkenrath, K. Hadjiyiannakou, K. Jansen, G. Koutsou, and A. Vaquero Aviles-Casco, *Phys. Rev. D* **100**, 014509 (2019), [arXiv:1812.10311 \[hep-lat\]](#).
- [88] D. Djukanovic, G. von Hippel, H. B. Meyer, K. Ottnad, M. Salg, and H. Wittig, (2023), [arXiv:2309.06590 \[hep-lat\]](#).
- [89] A. D. Martin, W. J. Stirling, R. S. Thorne, and G. Watt, *Eur. Phys. J. C* **63**, 189 (2009), [arXiv:0901.0002 \[hep-ph\]](#).
- [90] J. Holligan and H.-W. Lin, (2023), [arXiv:2312.10829 \[hep-lat\]](#).